Journal of Statistical Physics, Vol. 39, Nos. 5/6, 1985

Multifluxon Dynamics in Driven Josephson Junctions

Albert Lawrence,[1] Nung Soo Kim,[1] James McDaniel,[2] and Michael Jack[2]

The dynamics of fluxons in a long Josephson junction driven by time-varying nonuniform bias currents are described by a generalization of the sine-Gordon equation. This equation has solitary wave solutions which correspond to current vortices or quantized packets of magnetic flux in the junction. As with the sine-Gordon equation, multifluxon solutions may be demonstrated for the long Josephson junction. Our numerical calculations show that several fluxons may be launched or annihilated at the end of a junction. We also show multiple steady state conditions which correspond to one or more flux quanta trapped in the junction.

KEY WORDS: Josephson transmission line; solitary wave; fluxon; sine-Gordon equation; numerical model.

1. PHYSICS OF THE LONG JOSEPHSON JUNCTION

Although a number of configurations are possible, a Josephson junction is most often fabricated as a thin dielectric layer (30–100 A) separating two superconductors.[1] Because of the formation of Cooper pairs, the electons in a superconductor share a common phase.[1,2] The phase, current, and voltage across the dielectric in a Josephson junction are given by the Josephson relations:

$$\partial\varphi/\partial t = 2eV/h \tag{1}$$

$$j = J_c \sin(\varphi) \tag{2}$$

where φ is the phase, J_c is the critical current, and V is the voltage across the junction.[1,2] A Josephson junction is called a Josephson transmission

[1] Hughes Aircraft Company, 6155 El Camino Real, Carlsbad, California, 92008.
[2] Hughes Aircraft Company, P. O. Box 9399, Long Beach, California, 90810.

0022-4715/85/0600-0563$04.50/0

line or long Josephson junction if the length of the junction is large in comparison to the coherence length. The coherence length λ_J is given by the formula

$$\lambda_J = (\hbar c^2/8\pi e d J_c)^{1/2} \tag{3}$$

where c is the speed of light, e is the electron charge, and d is the total magnetic penetration depth.[1]

Under proper conditions, discrete packets of magnetic flux (fluxons) may be caused to propagate along the junction. These packets, induced by minute current vortices, behave as solitary waves, and exhibit particlelike properties.[1,3–15] The nonuniform current flow may be related to a difference in Josephson phase, $\varphi(x, t)$, across the junction or to a nonuniform magnetic field $B(x, t)$ within the barrier region. We follow Fulton's treatment.[3]

In order to derive the evolution equations for the Josephson phase, we first relate the phase and voltage by means of a contour integral as in Fig. 1. We assume that the superconductors are thick in comparison to the penetration depth of the magnetic field and that the portion of the contour parallel to the barrier is placed beyond the penetration depth of the magnetic field in the superconducting electrodes. In this case, the only significant contribution to the integral is over the portion of the curve which crosses the barrier. In particular,

$$V(x_2) - V(x_1) = d\Phi/dt \tag{4}$$

where Φ is the flux linking the curve. Integrating over time we obtain the relation

$$\varphi(x_2) - \varphi(x_1) = 2\pi\Phi/\Phi_0 \tag{5}$$

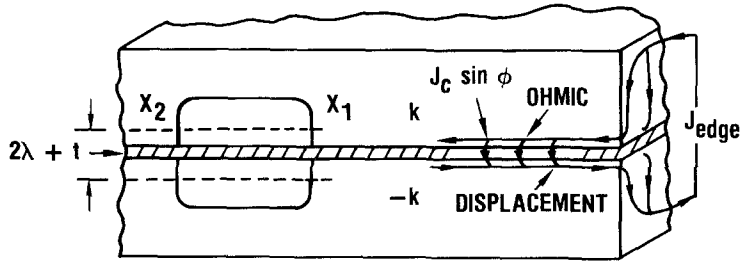

Fig. 1. Cross section of a Josephson junction. Penetration depth = . Contour of integration is between x and x, k is current parallel to junction.

Taking the limit as x_2 approaches x_1, and noting that the magnetic field is confined within the barrier region we obtain

$$\partial\varphi/\partial x = (2\pi\mathbf{d}/\Phi_0)\, B_y \tag{6}$$

where $\mathbf{d} = 2 + \mathbf{t}$. The magnetic field $B_y(x, t)$ induces currents as shown in Fig. 1. Letting $k(x, t)$ denote the current density, we have

$$k = B_y/\mu_0 \tag{7}$$

Using Eqs. (5) and (6), we see

$$\begin{aligned}\partial k/\partial x &= (2\pi\mathbf{d}\mu_0/\Phi_0)^{-1}\, \partial^2\varphi/\partial x^2 \\ &= J_c \sin(\varphi) + \sigma V + (\varepsilon_0\kappa/\mathbf{t})(\partial V/\partial t) + I_{\text{edge}} \\ &= J_c \sin(\varphi) + (\sigma\Phi_0/2\pi)\, \partial\varphi/\partial t + (\varepsilon_0\kappa\Phi_0/2\pi\mathbf{t})\, \partial^2\varphi/\partial t^2 + I_{\text{edge}}\end{aligned} \tag{8}$$

We may rewrite Eq. (8) in the form presented by Fulton (3):

$$K_l\, \partial^2\varphi/\partial x^2 = J_c \sin(\varphi) + D_l\, \partial\varphi/\partial t + M_l\, \partial^2\varphi/\partial t^2 + I_{xl} \tag{9}$$

where J_c = critical current density, I_{xl} = bias current density, $K_l = \Phi_0/2\pi L_l$, L_l = inductance (per unit length), $M_l = \Phi_0 C_l/2\pi$, $D_l = w\Phi_0/2\pi$, and C_l = capacitance (per unit length).

The dynamics of in a Josephson junction may be described by a sine-Gordon equation with additional terms for dissipation and driving currents. Generally, time and space variables are normalized so the equation becomes

$$\varphi_{xx} - \varphi_{tt} - \sin(\varphi) = \alpha\varphi_t - \gamma \tag{10}$$

(See Refs. 10, 13, and 15.) Additional dissipative terms may be added to the equation. The effects of surface impedance, given by a term $-\beta\varphi_{xxt}$, are investigated in Refs. 11, 12, and 14. Although the general features of multifluxon dynamics reported in those references are similar to those given by Eq. (10), fluxons tend to "bunch" (11) rather than to repel one another. Assumption of a quadratic dissipation term $|\varphi_t|^2$, rather than the linear dissipation terms, permits an analytic solution for steady state fluxon propagation[9] and produces qualitative agreement between the model and experimentally observed current–voltage curves for long junctions.

Because dissipation terms are generally small in magnitude, many of the most interesting properties of freely propagating fluxons are closely related to the properties of soliton solutions of the pure sine-Gordon equation.[8] The literature associated with the pure sine-Gordon equation is

quite extensive. Reviews may be found in recent books by Lamb[16] and by Dodd, Eilbeck, Gibbon, and Morris.[17] Solutions of the pure sine-Gordon equation may be found by separation of space and time variables.[16] Generalizations of this technique yield multisoliton solutions which may be expressed in terms of the Jacobi theta functions[18] and the Riemann-theta functions.[19–23] Solutions for the sine-Gordon equation generalized to two or more spatial dimensions are also given in terms of the Riemann theta functions.[19–23] An alternative approach to multisoliton dynamics is through inverse scattering theory.[16,17,24]

Experimental evidence of fluxons in Josephson junctions is also extensive. Reported work includes observation of zero-field steps in the current–voltage characteristics of the junction,[9,13–15,25] measurement of millimeter wave radiation generated by fluxons reflecting from the ends of the junction,[11,26–28] obsrvation of fluxons by laser scanning,[29] and direct measurement of the voltage pulses induced by propagating fluxons.[5,6,30,31]

Applications for the long Josephson junction to both analog and digital circuitry have been proposed in the physics and engineering literature. The analog applications include use of the long Josephson junction as a high frequency oscillator. One or more fluxons repeatedly reflecting from the ends of a long junction constitute a source of millimeter and submillimeter wave radiation.[4,26,28,32–35] Although reported power levels are presently one microwatt or less,[28] radiation linewidths and tuning ranges make the long Josephson junction oscillator an attractive device for future development—especially in the 200–1000-GHz range.[26] Long Josephson junctions may also be fabricated in a ring configuration.[5] These devices have been proposed as accelerometers.[36]

Several applications to digital logic have also been proposed.[37–39] The long Josephson junction may be used as a three-terminal device having the analogs of the source, gate, and drain of a transistor.[40,41] Voltage amplification factors in this device may approach 100 or better. Single fluxons may also be transmitted as bits of information in circuits based on Josephson transmission lines. Several architectures based on Josephson junction processors have been proposed for digital memories and processors.[38,39]

2. THE TRANSMISSION LINE MODEL

The model of Erne and coworkers may be easily generalized to the case of nonuniform junction parameters. We assume that the quantities R_l, C_l, L_l, J_l, and I_{xl} in the Fulton model (3) are replaced by functions $R(x)$, $C(x)$, $L(x)$, $J(x)$, and $I_B(x, t)$. The continuous case with spatially varying parameters may be approximated by a simple network, as in Fig. 2.

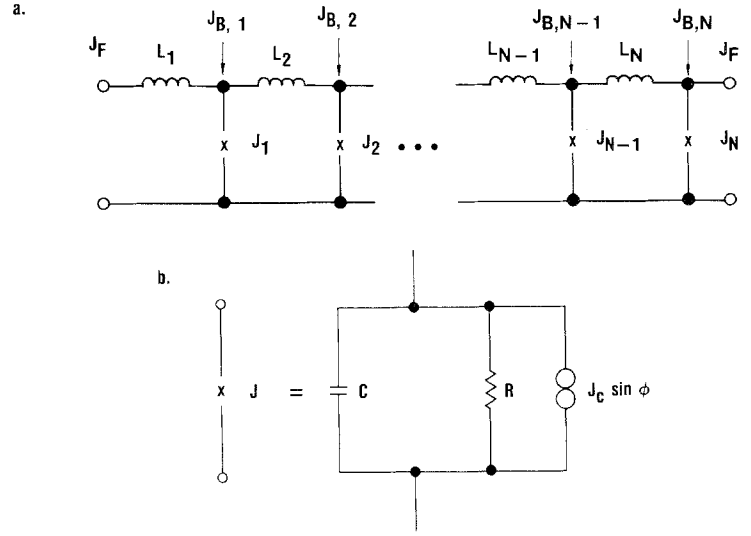

Fig. 2. (a) Lumped circuit approximation for a long Josephson junction. J_F is field-induced current, $J_{B,i}$ is bias current. (b) Fulton model for point junction. C is junction capacitance, R is resistance (to quasiparticle tunneling), $J\sin(\varphi)$ is the supercurrent.

In this figure, R_i, C_i, L_i, and J_i represent the lumped characteristics of the ith segment (of length x). The quantity $J_{B,i}(t)$ represents the total bias current applied to the ith segment, and $J_F(t)$ represents the effect of a uniform magnetic field. Although this model represents an overlap junction, as in Fig. 3a, trivial modifications serve to represent an in-line configuration, or the effects of nonuniform magnetic fields, which might be induced by control lines. The equations for this model are a generalization of the equations of Erne and Parmentier[33]:

$$\begin{aligned} C(dV_1/dt) &= (\Phi_0/2\pi L_2)(\varphi_2 - \varphi_1) - V_1/R_1 - J_1 \sin(\varphi_1) + J_{B,1} + I_F \\ C(dV_i/dt) &= (\Phi_0/2\pi)[(1/L_i)\,\varphi_{i-1} - (1/L_{i+1} - 1/L_i)\,\varphi_i \\ &\quad + (1/L_{i+1})\,\varphi_{i+1}] - V_i/R_i - J_i \sin(\varphi_i) + J_{B,i} \\ C(dV_N/dt) &= (\Phi_0/2\pi L_N)(\varphi_{N-1} - \varphi_N) - V_N/R_N - J_N \sin(\varphi_N) + J_{B,N} - I_F \end{aligned} \tag{11}$$

In these equations N represents the number of junction segments in the model. These equations may be derived from the Josephson relations [Eqs. (1)] and the current and voltage balance equations for the network. An alternative approach would be to discretize the spatial variable in Eq. (9), using standard difference approximations for the spatial derivatives. Both procedures yield the same results. For purposes of

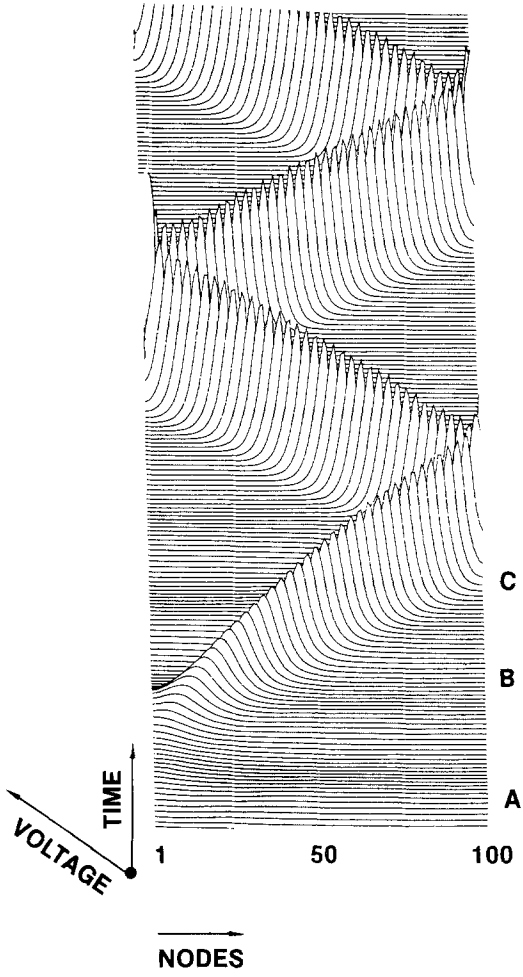

Fig. 3. Generation and propagation of a single fluxon. Junction parameters are as in the text. Horizontal axis represents distance along the junction, while voltage and time are superimposed on the vertical axis. Horizontal traces are at 1-psec intervals. A current pulse having maximum amplitude 3.8 times critical current density is applied to the first two nodes at beginning of the record. Pulse shape is trapezoidal, 10 psec linear increase, 10 psec at maximum, and 10 psec decrease to bias. Bias current is 0.6 times critical current density at all nodes and at all times except when initial current pulse is applied. A field-induced current at 0.9 times critical current density is assumed at the first and last nodes (see Fig. 1). A, Application of current pulse; B, fluxon is accelerated to limit velocity; C, fluxon reflects from end of junction.

numerical computation, we set $N = 200$ and used the junction parameters $R_i = 20\,\Omega$, $C_i = 10^{-12}$ F, $L_i = 6 \times 10^{-14}$ H, and $J_i = 10^{-4}$ A. These parameters correspond to characteristics readily achievable in $2\,\mu \times 2\,\mu$ lead–lead oxide–lead junctions.

The bias current was the only independent variable in the model.

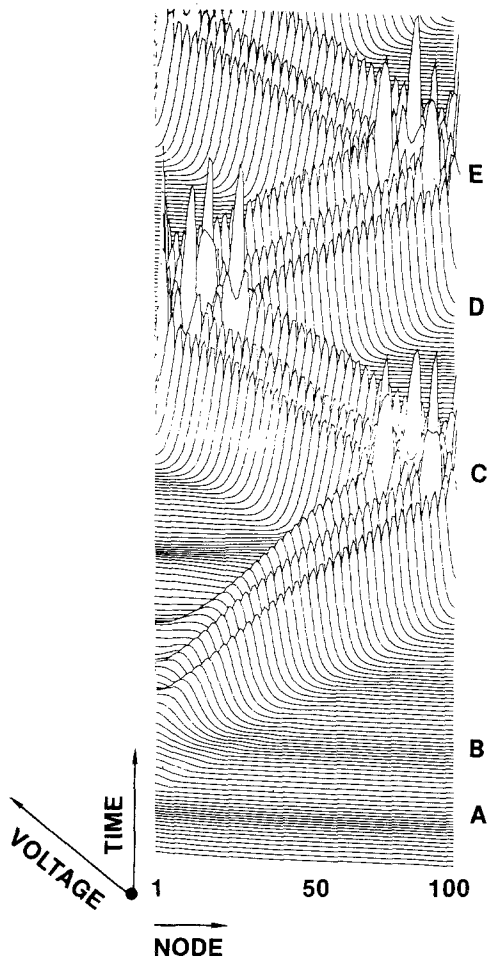

Fig. 4. Generation and propagation of a train of three fluxons. Model parameters as given in Fig. 3, except current pulse maximum is 5.0 times critical current density. A, current pulse; B, formation of three fluxons; C, D, E, fluxons reflect from ends of junction. Note that fluxons emerge from interactions without change in shape.

Various functions for bias current input were selected during the course of our computations, as will be described in the next section. The resulting equations, with time- and space-varying bias currents, were solved numerically on a VAX 11/780 computer, using the code developed by Shampine and Gordon.[42]

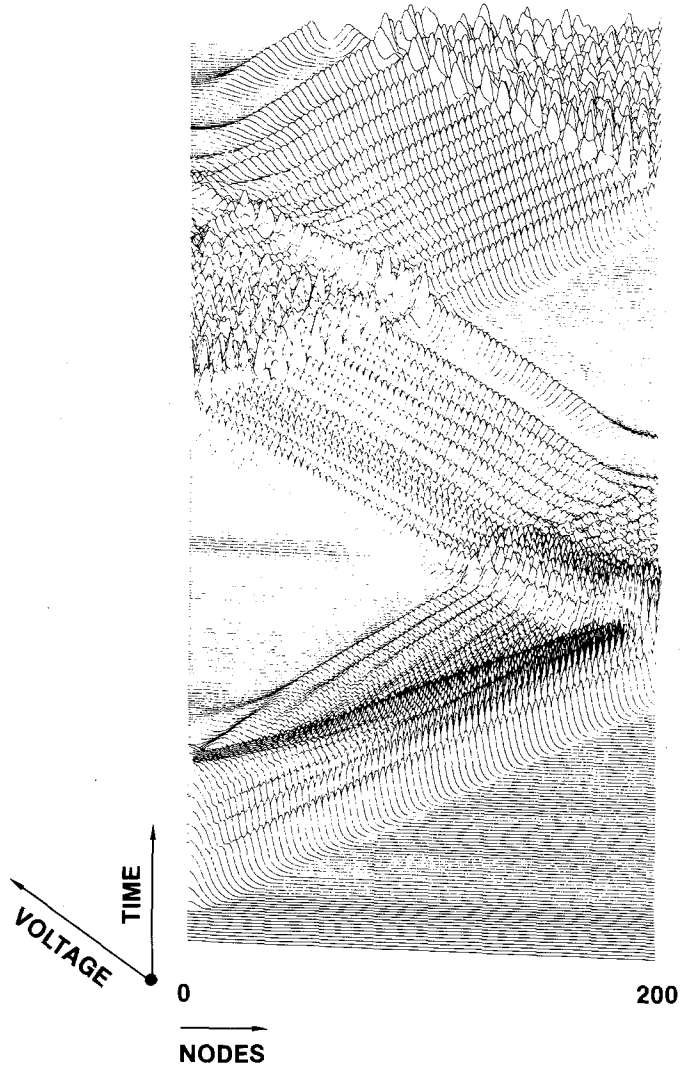

Fig. 5. Generation and propagation of a "lump" containing 32 fluxons. Note that all but 16 fluxons are lost through dissipative processes at the ends of the junction. This model differs from the one used for Figs. 3 and 4 in that junction length is 400 μ (200 nodes).

3. RESULTS

Single fluxons, multiple fluxons, and "lumps" containing large numbers of flux quanta may be induced by application of current pulses to the end of a junction. Figures 3 through 5 are records of the voltage across the junction. Each trace is separated by 1 psec. Figure 3 shows a single fluxon, Fig. 4 three fluxons, and Fig. 5 a shock-wave containing 32 fluxons. In each case, the bias current pulse was applied to the first two nodes about 10 psec after the beginning of the record. Except for the period of 30 psec, during which the fluxon-inducing current pulse was applied, the bias was maintained at 0.6 times the critical current density along the entire junction.

Generally, individual fluxons in a train of fluxons tended to remain at least 25 μ apart, as may be seen by reference to Fig. 4. Furthermore, the trailing fluxons in a train were seen to lag, as may also be seen in Fig. 4. The lagging of the trailing fluxons seems to be more pronounced if larger numbers of fluxons are present in the junction. This may be seen by comparing Figs. 4 and 5. If more flux quanta were introduced at the end of the junction than the junction could accomodate at 25 μ separation, the sur-

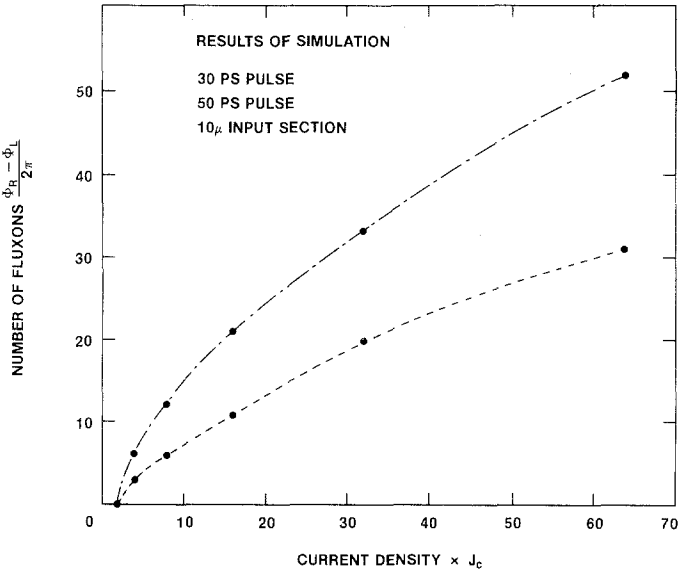

Fig. 6. Relation between input current pulse and number of fluxons produced. Horizontal axis is maximum current density normalized to critical current density. Vertical axis is phase difference between the right and left ends of the junction divided by 2. Phase difference is measured 50 psec after cessation of input current pulse.

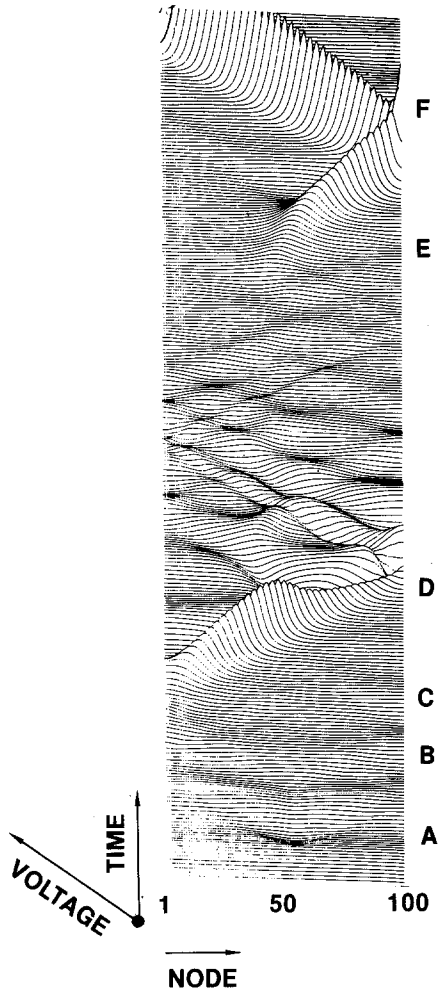

Fig. 7. Trapping and release of a single fluxon. A: Establishment of a negative bias on center section, nodes 50–59 of the model. Magnitude of the current is 3.0 times critical current density. Bias on remainder of the junction is as in Fig. 3. B–C: Current pulse. D: Single fluxon is trapped at center section. E: Negative bias is reversed to +0.6 times critical current density. F: Fluxon reflects from end of junction.

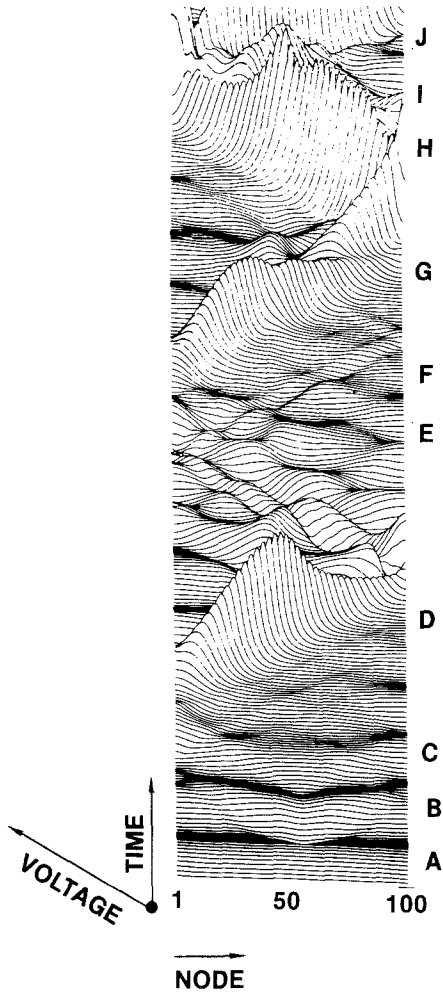

Fig. 8. Interaction of a trapped and a propagating fluxon. A–D: See Fig. 7. E–F: Second current pulse. G: Second fluxon collides with trapped fluxon. H: Fluxon emerges at right side of trapping section and reflects from end of junction. I: Second fluxon collides with trapped fluxon again. J: Fluxon emerges at left side of trapping section. Process continues indefinitely.

plus flux quanta were lost at the opposite end of the junction. This may be seen in Fig. 5.

We also obsrved that under the constant bias current condition single fluxons accelerated to a limiting velocity and the associated voltage pulse increased to a limiting amplitude. This is predicted by the perturbation theory[7] which gives the formula

$$v_\infty = [1 + (4\alpha/\pi\gamma)^2]^{-1/2} \tag{12}$$

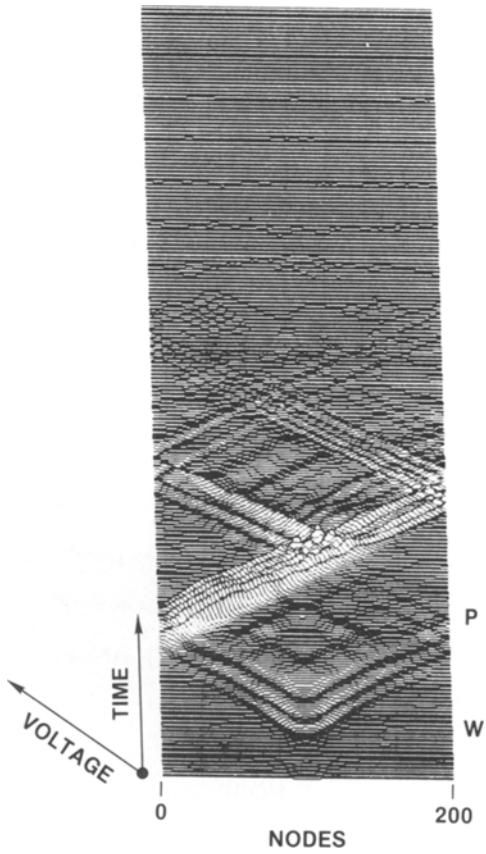

Fig. 9. Trapping multiple fluxons. W: Negative bias established on nodes 90–110 of the model. Magnitude of bias current is 3.0 times critical current density. P: 50-psec current pulse, at 60 psec after beginning of record. Pulse is administered to first five nodes of the model, and is trapezoidal, 10-psec increase, 30 psec at maximum, 10-psec decrease. Bias on junction is 0.6 times critical current density, except at initial section during current pulse, and at center negative bias section. Five fluxons are produced and trapped at center of junction. Note oscillations which scatter from negative bias section during collision of fluxons.

The lagging of the trailing fluxons during the time interval when they are leaving the end of the junction seems also to be a result of this relation. This is because bias currents are effectively reduced near the end of the junction after the lead fluxons in a train have reflected from the end of the junction.

The number of fluxons generated by a current pulse is not generally a linear function of the current delivered. Figure 6 shows the number of fluxons generated under various conditions. The relation is approximately parabolic.

We have also observed that one or more fluxons may be trapped by a region of negative bias. Figure 7 illustrates the capture and release of a single fluxon, while Fig. 8 shows the interaction between a fluxon trapped at 100 psec and a second fluxon which is induced by a current pulse 100 psec later. Although the pattern of interaction is rather complex, the second fluxon propagates through the first. This was verified by calculating

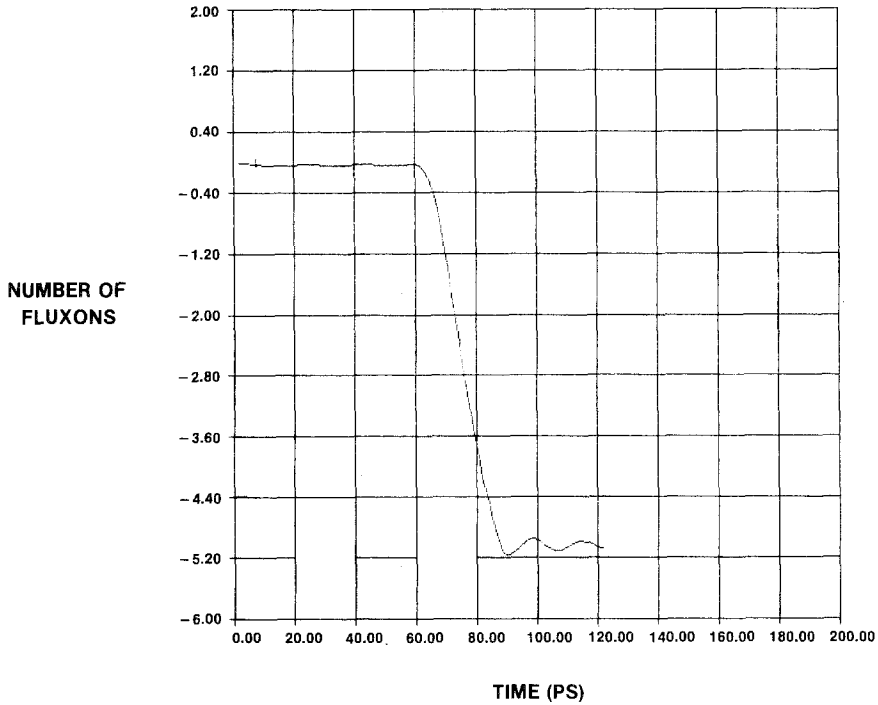

Fig. 10. Phase difference between ends of junction during process shown in Fig. 9. Horizontal axis is time, vertical axis is number of fluxons in the junction (phase difference across the junction divided by 2). The number stabilizes at five fluxons, after scattered oscillations dissipate.

of the time-varying magnetic field (not shown). The length of the section over which the bias current is applied is 20 μ, and the magnitude of the negative bias is 3.0 times critical current density in both cases.

Increasing the length of the section over which the negative bias is induced makes trapping of several flux quanta possible. Figures 9 and 10 show the voltage along the junction, and 1/2 times the phase difference

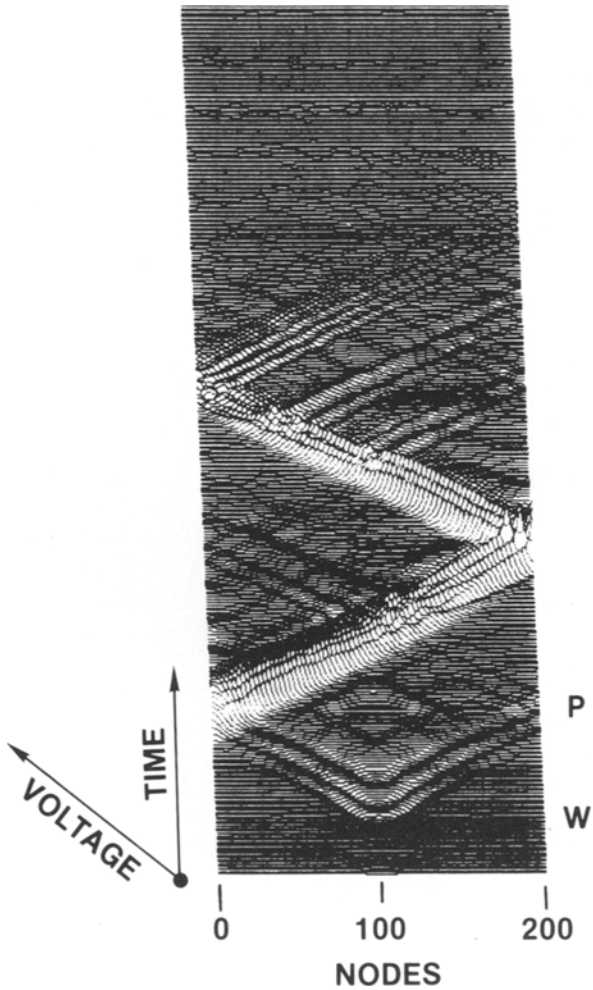

Fig. 11. Production of 11 fluxons by current pulse, followed by loss at junction end. W and P mark the same events as in Fig. 9 except that current pulse is 19.0 times critical current density. Note that several fluxons propagate through junction before dissipating to the right of the trapping section.

between the ends of the junction. As may be seen from Fig. 10, five flux quanta are produced and remain on the junction. Figures 11 and 12 show the result of inducing seven fluxons. Five are trapped, and two are lost at the end of the junction. The loss seems to be a function of the total momentum of the flux, because Figs. 13 and 14 show that at least ten flux quanta may be trapped, if they are produced five at a time. In each of these cases the negative bias current section is 60 μ and the magnitude of the current density is 3.8 times critical.

One interesting aspect of a long Josephson junction which emerges from the numerical calculations (as exemplified by Figs. 9–14) is that it can have multiple stable states. This is distinguished from the case of a system with pure sine-Gordon dynamics which, because its solitons repel one another, cannot have a multisoliton stable state.

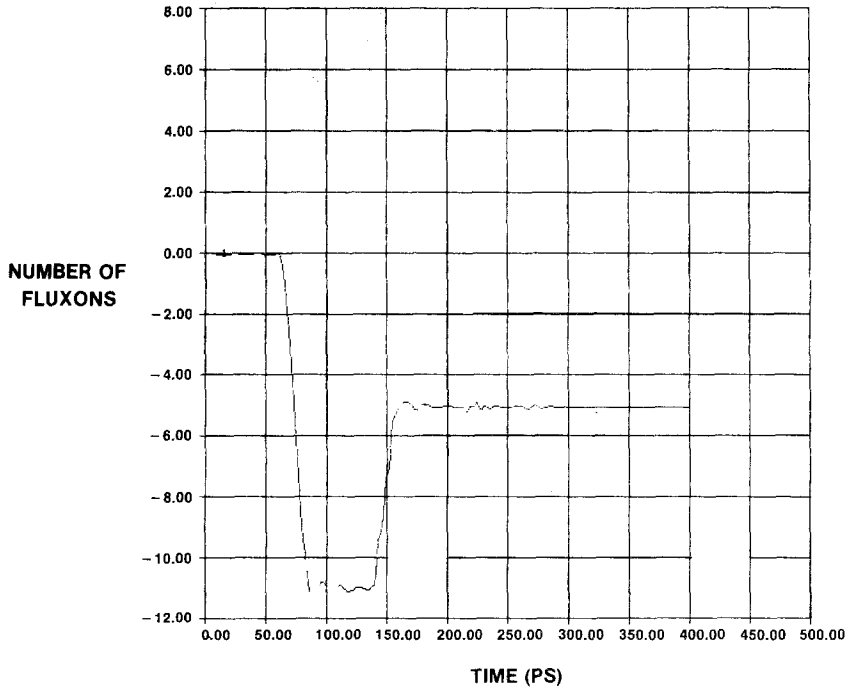

Fig. 12. Phase difference between ends of the junction during process shown in Fig. 11. Record stabilizes at five fluxons.

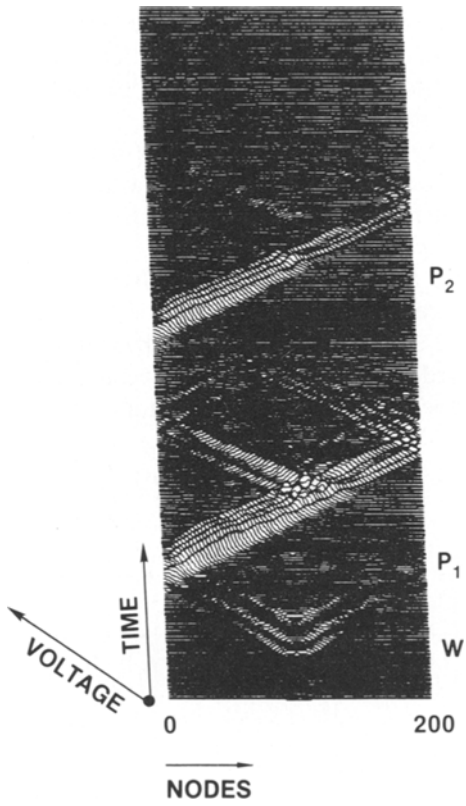

Fig. 13. Trapping fluxons in two stages. W and P_1 represent the same process as in Fig. 9. P_2: A second pulse is applied to the junction, at 100 psec after first pulse, generating an additional five fluxons.

4. DISCUSSION

The findings of main significance in this numerical study center around the trapping of flux at a region of negative current bias. Because trapped flux corresponds to a stationary state of the phase function, capacitative and dissipative currents are zero. This implies that the only currents in a stationary state are supercurrents along the electrodes and across the barrier. The inductance of the counter electrode is much greater than of the base in the overlap geometry chosen for our study. For this reason, trapped flux corresponds to increased currents parallel to the junction in the counter electrode. In particular, the trapping of one or more fluxons moving from the left results in a larger current entering the left boundary of the negative bias section. Thus, the number of fluxons which could be trapped

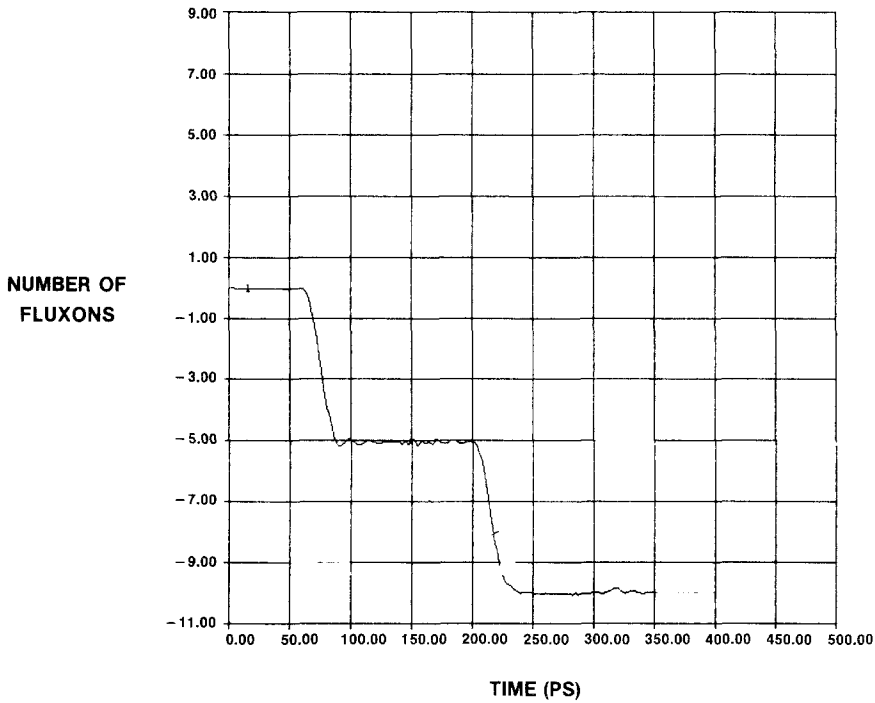

Fig. 14. Phase difference record corresponding to the process of Fig. 13. Note that a total of ten fluxons are trapped at the center of the junction.

at the negative bias section is limited by the current which can enter the junction in the left positive bias section, or by the current which can leave the junction in the negative bias section, whichever is smaller. One may may make rough estimates of the upper limit by noting that the total Josephson current traversing the junction in the positive bias section will not generally contribute a significant portion of the current flowing along the counter electrode into the negative bias section.

The precise solution of the problem is to find all solutions of the equation

$$\varphi_{xx} = \sin(\varphi) - \gamma \tag{13}$$

subject to the constraints

$$\begin{aligned} &\int_0^l [\sin(\varphi) - \gamma]\, dx = 0 \\ &(1/2\pi) \int_0^l \varphi_x\, dx = 0, 1, \ldots, n \end{aligned} \tag{14}$$

where n may be the upper limit calculated from the bias current.

If we have found a solution to Eq. (11), then a small perturbation, $\delta\varphi$, will satisfy the equation

$$u_{xx} - u_{tt} = u\cos(\varphi) + \alpha u_t \tag{15}$$

where $u(x, 0) = \delta\varphi$. This shows that small disturbances tend to be damped out, so stationary solutions are stable.

The structural perturbation theory of McLaughlin and Scott predicts the trapping of fluxons by microshorts.[7] This study has shown that fluxons may also be trapped by regions of negative bias current. In addition, fluxons may be created or annihilated at the ends of a junction by control of the bias currents. These phenomena are susceptible to practical application, as suggested by Likharev *et al.*[41] and Nakajima *et al.*[38]

REFERENCES

1. A. Barone and G. Paterno, *Physics and Applications of the Josephson Effect* (Wiley–Interscience, New York, 1982).
2. D. Rogovin and M. Scully, *Phys. Rep.* **25**:175 (1975).
3. T. A. Fulton, in *Superconductor Applications*, B. B. Schwartz and S. Foner, eds. (Plenum Press, New York), pp. 125–187.
4. A. C. Scott, *Solid State Electron.* **7**:137 (1964).
5. A. C. Scott and S. A. Reibel, *J. Appl. Phys.* **46**:4935 (1975).
6. A. C. Scott, F. Y. F. Chu, and S. A. Reibel, *J. Appl. Phys.* **47**:3272 (1975).
7. D. W. McLaughlin and A. C. Scott, *Phys. Rev. A* **18**:1652 (1978).
8. G. Costable, R. D. Parmentier, B. Savo, D. W. McLaughlin, and A. C. Scott, *Appl. Phys. Lett.* **32**:587 (1978).
9. R. D. Parmentier and G. Costabile, *Rocky Mtn. J. Math.* **8**:117 (1978).
10. P. L. Christiansen and O. H. Olsen, *Wave Motion* **2**:185 (1980).
11. P. L. Christiansen, P. S. Lomdahl, A. C. Scott, O. H. Soerensen, and J. C. Eilbeck, *Appl. Phys. Lett.* **39**:108 (1981).
12. V. I. Karpman, N. A. Ryabova, and V. V. Solov'ev, *Phys. Lett.* **85A**:251 (1981).
13. O. A. Levring, N. F. Pedersen, and M. R. Samuelsen, *Appl. Phys. Lett.* **40**:846 (1982).
14. P. S. Lomdahl, O. H. Soerensen, and P. L. Christiansen, *Phys. Rev. B* **25**:5737 (1982).
15. N. F. Pedersen and D. Welner, *Phys. Rev. B* **29**:2551 (1984).
16. G. L. Lamb, Jr., *Elements of Soliton Theory* (Wiley–Interscience, New York, 1980).
17. R. K. Dodd, J. C. Eilbeck, J. D. Gibbon, and H. C. Morris, *Solitons and Nonlinear Wave Equations* (Academic Press, New York, 1982).
18. E. D. Belokolos and V. Z. Enol'skii, *Theor. Math. Phys.* **53**:1120 (1983).
19. J. Zagrodinski, *Lett. Nuovo Cimento* **30**:266 (1981).
20. J. Zagrodinski, *J. Phys. A* **15**:3109 (1982).
21. J. Zagrodinski and M. Jaworski, *Z. Phys.* **B49**:75 (1982).
22. J. Zagrodinski, *J. Math. Phys.* **24**:46 (1983).
23. J. Zagrodinski, *Phys. Rev. B* **29**:1500 (1984).
24. M. G. Forest and D. W. McLaughlin, *J. Math. Phys.* **23**:1248 (1982).
25. M. Radparvar and E. Nordman, Applied Superconductivity Conference, November 30–December 3, Knoxville, Tennessee (1983).

26. M. Salerno and A. C. Scott, *Phys. Rev. B* **26**:2474 (1982).
27. M. Scheuermann, J. T. Chen, and J.-J. Chang, *J. Appl. Phys.* **54**:3286 (1983).
28. T. Nagatsuma, K. Enpuku, F. Irie, and K. Yoshida, *J. Appl. Phys.* **54**:3302 (1983).
29. J. R. Lhota, M. Scheuermann, P. K. Kuo, and J. T. Chen, Applied Superconductivity Conference, November 30–December 3, Knoxville, Tennessee (1982).
30. A. Matsuda and S. Uehara, *Appl. Phys. Lett.* **41**:770 (1982).
31. J. Nitta, A. Matsuda, and T. Kawakami, *J. Appl. Phys.* **55**:2758 (1984).
32. A. C. Scott, in *Solitons and Condensed Matter*, A. R. Bishop and T. Schneider, eds. (Springer-Verlag, New York, 1978), pp. 301–311.
33. S. N. Erne and R. D. Parmentier, *J. Appl. Phys.* **51**:5025 (1980).
34. P. S. Lomdahl, O. H. Soerensen, P. L. Christiansen, A. C. Scott, and J. C. Eilbeck, *Phys. Rev. B* **24**:7460 (1981).
35. S. N. Erne, A. Ferrigno, S. Di Genova, and R. D. Parmentier, *Lett. Nuovo Cimento* **34**:121 (1982).
36. P. Russer, *AEÜ (Archiv für Elektronic und Übertragungstechnik)* **37**:153 (1983).
37. H. S. Newman and K. L. Davis, *J. Appl. Phys.* **53**:7026 (1982).
38. K. Nakajima, G. Oya, and Y. Sawada, Applied Superconductivity Conference, November 30–December 3, Knoxville, Tennessee (1982).
39. T. V. Rajeevakumar, Applied Superconductivity Conference, November 30–December 3, Knoxville, Tennessee (1982).
40. K. K. Likharev, Applied Superconductivity Conference 76, 242–244, 245–247 (1976).
41. K. K. Likharev, V. K. Semenov, O. V. Snigirev, and B. N. Tedorov, ASC 78, 420–423 (1978).
42. L. F. Shampine and M. K. Gordon, *Computer Solution of Ordinary Differential Equations* (W. H. Freeman and Company, San Francisco, 1975).